

^1H and ^{27}Al NMR study of the ferroelectric transition in dimethylammonium aluminum sulphate hexahydrate $(\text{CH}_3)_2\text{NH}_2\text{Al}(\text{SO}_4)_2 \cdot 6\text{H}_2\text{O}$

J. Dolinšek, M. Klanjšek, D. Arčon, Hae Jin Kim,* J. Seliger, and V. Žagar
J. Stefan Institute, University of Ljubljana, Jamova 39, SLO-1000 Ljubljana, Slovenia

L. F. Kirpichnikova

Shubnikov Institute of Crystallography, Russian Academy of Sciences, Leninskii prospect 59, Moscow, 117333 Russia

(Received 18 March 1998; revised manuscript received 18 September 1998)

Dimethylammonium aluminum sulphate hexahydrate $(\text{CH}_3)_2\text{NH}_2\text{Al}(\text{SO}_4)_2 \cdot 6\text{H}_2\text{O}$ (DMAAS) is a representative of a family of inorganic hydrogen-bonded insulators with a complicated structure of the H-bond network. The microscopic nature of the ferroelectric phase transition at $T_c = 152$ K was studied via the ^1H and ^{27}Al NMR spectrum, spin-lattice relaxation, and relaxation in the dipolar frame. Two kinds of molecular motions were detected in the paraphase with frequencies differing for about five orders of magnitude. The slow motion corresponds to the dimethylammonium (DMA) reorientational dynamics that freezes out at the ferroelectric transition whereas the fast motion reflects the dynamics of the H-bond network, which shows no anomaly at T_c . The results demonstrate that the DMA reorientation freeze-out is the prime reason for the ferroelectric transition in DMAAS. The DMA slowing-down dynamics has a profound effect on the other two sublattices of the DMAAS structure, the SO_4 and the $\text{Al}(\text{H}_2\text{O})_6$, via the hydrogen bonding. The effect of the relatively slow DMA reorientations is a gradual lowering of the time-average local crystal symmetry which biases the local potentials of water molecules in the $\text{Al}(\text{H}_2\text{O})_6$ complexes as well as the potentials of the H bonds. The gradual freeze-out of the water "jump-over" motion seems to be responsible for the appearance of four minima in the ^{27}Al spin-lattice relaxation rate in the paraphase which appear in addition to the global minimum at the ferroelectric transition. The splitting of the ^{27}Al spectral lines much below the ferroelectric transition temperature indicates that proton ordering in the H bonds begins to take place below 90 K. [S0163-1829(99)11105-6]

I. INTRODUCTION

Hydrogen-bonded insulating crystals represent a class of solids which exhibit many interesting physical phenomena like ferroelectricity, ferroelasticity, superionic conductivity and glassy ordering in the ferroelectric-antiferroelectric mixtures. In these systems hydrogen bonds connect different structural elements of the crystalline lattice and the above phenomena are crucially related to the structure and dynamics of the H-bond network. Physical properties of H-bonded crystals are strongly related to the dimensionality of the H-bond network. The simplest case is the $\text{K}_3\text{H}(\text{SO}_4)_2$ family in which a "zero-dimensional" H-bond network (isolated $\text{SO}_4\text{-H}\cdots\text{SO}_4$ dimers) exist. The dimensionality of the network is increased in CsHSO_4 family which contains one-dimensional (1D) H-bonded chains of SO_4 tetrahedra. In squaric acid the H-bond network is two-dimensional (2D), whereas in KH_2PO_4 (KDP) family a three-dimensional (3D) network exists where all four apices of a given PO_4 tetrahedron are H-bonded to other tetrahedra. All the above networks are geometrically still rather simple. For instance, the 3D KDP network is a stack of 2D H-bonded planes, where in each plane there exist two sets of orthogonal 1D H-bonded chains. The physical properties of the above systems can be to a good approximation modeled by considering the statics and dynamics of the H-bond network only, whereas the effect of the rest of the crystalline lattice can be considered as minor.

Recently a new family of H-bonded inorganic insulators has been discovered where the dimension of the H-bond network is still 3D, but has a considerably more

complicated structure than in KDP. These are the dimethylammonium aluminum sulphate hexahydrate^{1,2} $(\text{CH}_3)_2\text{NH}_2\text{Al}(\text{SO}_4)_2 \cdot 6\text{H}_2\text{O}$ (DMAAS), the dimethylammonium gallium sulphate hexahydrate³⁻⁵ $(\text{CH}_3)_2\text{NH}_2\text{Ga}(\text{SO}_4)_2 \cdot 6\text{H}_2\text{O}$ (DMAGaS) and their deuterated forms. These crystals exhibit ferroelectricity and ferroelasticity. The microscopic nature of the above phenomena is still poorly understood due to a high complexity of the crystalline structure and the H-bonding network. There are three basic structural elements in DMAAS (Fig. 1). First are the $[\text{Al}(\text{H}_2\text{O})_6]^{3+}$ complexes which form regular octahedrons containing Al atom in the center and six water molecules in the apices. Each water molecule forms two strong $\text{O-H}\cdots\text{O}$ hydrogen bonds with the second structural elements, the $[\text{SO}_4]^{2-}$ anions. There are twelve H bonds between a given $\text{Al}(\text{H}_2\text{O})_6$ complex and the surrounding SO_4 tetrahedra, creating a rather complicated H-bond network. The combined $\text{Al}(\text{H}_2\text{O})_6\text{-SO}_4$ sublattice forms void channels inside which the third structural elements, the dimethylammonium $[(\text{CH}_3)_2\text{NH}_2]^+$ (DMA) cations are located. The DMA cations form two weak $\text{N-H}\cdots\text{O}$ hydrogen bonds between the amino (NH_2) group of the DMA molecule and the SO_4 tetrahedra. Two oxygen atoms of a given SO_4 molecule form two $\text{O-H}\cdots\text{O}$ bonds each with the Al complexes, whereas each of the remaining two oxygens forms one $\text{O-H}\cdots\text{O}$ bond with the Al complex and one $\text{N-H}\cdots\text{O}$ bond with the DMA molecule.

Ferroelastic properties^{6,7} of DMAAS and the ferroelectric (FE) phase transition^{1,2,8} at $T_c = 152$ K were discovered recently. At the FE transition the crystal symmetry changes from $2/m$ to m . The microscopic mechanism of the ferroelec-

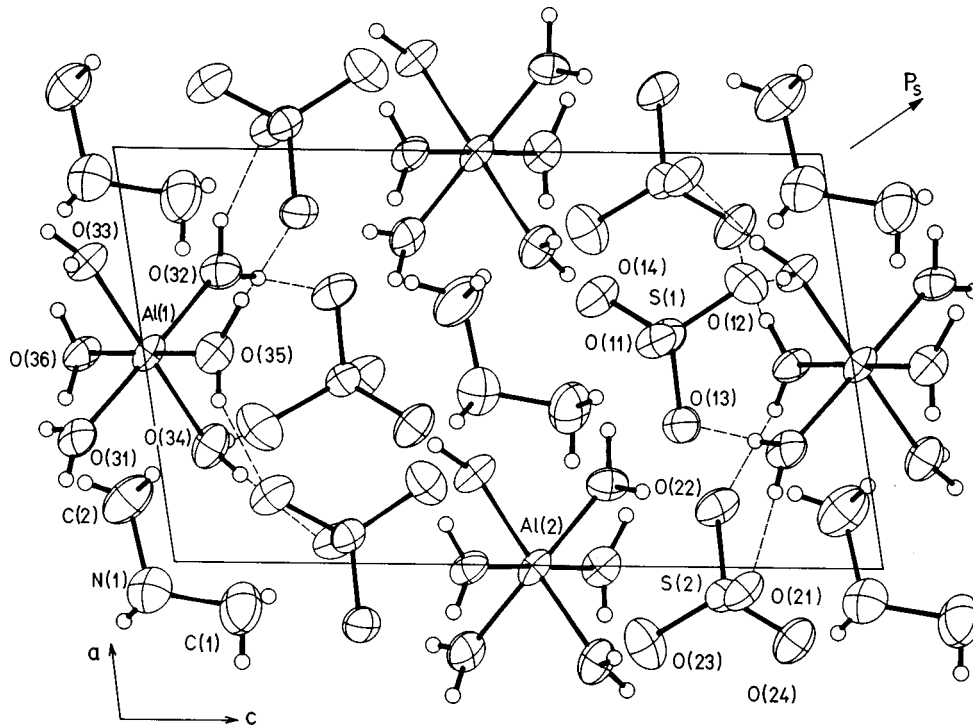


FIG. 1. A projection of the $(\text{CH}_3)_2\text{NH}_2\text{Al}(\text{SO}_4)_2 \cdot 6\text{H}_2\text{O}$ crystal structure onto the (a,c) plane in the ferroelectric phase (the notation of axes is taken from Ref. 1 with $a=0.6403$ nm, $b=1.0747$ nm, and $c=1.1128$ nm). The monoclinic (a,c) plane is the mirror plane and b is the twofold axis in the paraphase. The arrow shows the direction of the spontaneous polarization. One set of twelve O-H \cdots O bonds connecting a given $\text{Al}(\text{H}_2\text{O})_6$ complex with the SO_4 tetrahedra is shown (dashed lines).

tric ordering is still not understood. It is by now commonly accepted that the FE transition is of an order-disorder type, connected with the ordering of the DMA groups. At $T > T_c$ the DMA groups are dynamically disordered, executing random flips around the axis connecting the two methyl oxygens. This axis lies in the mirror (ac) plane of the paraelectric structure. X-ray study¹ has determined four equilibrium positions of the amino group, two realized with a probability 0.4 and the other two with 0.1. Below T_c the DMA molecules freeze in one position and the spontaneous dielectric polarization P_s occurs in the m plane. The direction of P_s is parallel to the vector joining the nitrogen atoms of the two DMA groups in the unit cell. The DMA group thus represents the basic reversible electric dipole and its ordering creates P_s below T_c .

Most spectroscopic studies of the FE transition in DMAAS like dielectric relaxation,^{1,9-11} sound velocity and specific heat,¹² considered the DMA ordering as the only reason for the occurrence of the ferroelectricity. The role of hydrogen bonding in the ferroelectric ordering was neglected, namely the possible freezing of the proton motion and the associated electrical polarization of the hydrogen bonds. Due to a complicated H-bonding scheme between all three building elements of the DMAAS structure it is however possible that the freezing of the proton motion and the DMA freeze-out are interrelated. It could be that the DMA freezing is not the prime reason for the phase transition but a consequence of the proton H-bond slowing-down dynamics. A definite answer to this question has not been obtained so far as a selective study of the proton motion has not been carried out as yet. The existing investigations were performed with the bulk spectroscopic techniques which could

not resolve the H-bond dynamics from the DMA motion. In this paper we present a local, site-specific study of the DMAAS dynamics using the NMR spectroscopy of ^1H and ^{27}Al nuclei where the DMA and the H-bond dynamics are observed separately, showing clearly their respective roles in the FE phase transition.

II. PROTON NMR RELAXATION

The dynamics of the DMAAS crystal can be conveniently studied by NMR relaxation techniques. The ^1H spin-lattice relaxation rate $(T_1)^{-1}$ probes the dynamics on the frequency scale of the nuclear spin precession (10^7 Hz). The ^1H relaxation rate in the dipolar frame $(T_{1D})^{-1}$ is, on the other hand, sensitive to much slower motions in the kHz range, so that it is possible to perform a “two-clock” experiment, where the dynamics of the investigated system is observed on two experimental time scales which differ by four orders of magnitude. In DMAAS such an experiment could provide a key to resolve the relatively fast H-bond dynamics from the considerably slower DMA cation reorientations.

In DMAAS there exist three kinds of protons, the O-H \cdots O, the N-H \cdots O, and the CH_3 , which are all coupled by the magnetic dipole interaction. In addition, the ^{27}Al nuclei have a rather strong magnetic dipole moment too, so that the coupling of protons to the ^{27}Al nuclei should be considered as well. Due to a complicated magnetic-dipole coupling scheme of a large number of nuclei we use instead of the exact dipole-dipole relaxation formulas the simpler model that the nuclei experience randomly fluctuating uncorrelated local magnetic fields created by their neighbors. Within this model we are able to make a simultaneous analysis of the T_1

and T_{1D} relaxation times in the “two-clock” experiment.

We assume that the DMAAS dynamics can be divided into two kinds of motions. First are the DMA cation reorientations which were shown to take place between four equilibrium positions.¹ Two of these have the energy E_α and the other two E_β ($E_\beta > E_\alpha$) with the Boltzmann occupation probabilities $W_i \propto \exp\{-E_i/k_B T\}$. The DMA reorientations are thus performed in an asymmetric potential with the bias energy $\Delta = E_\beta - E_\alpha$. In such a case one defines the population difference p

$$p = W_\alpha - W_\beta = \tanh\left(\frac{\Delta}{2k_B T}\right) \quad (1)$$

and writes the DMA reorientation rate τ_{DMA}^{-1} as a sum of the “up” $\alpha \rightarrow \beta$ rate (τ_\uparrow^{-1}) and the “down” $\beta \rightarrow \alpha$ rate (τ_\downarrow^{-1})

$$\frac{1}{\tau_{\text{DMA}}} = \frac{1}{\tau_\uparrow} + \frac{1}{\tau_\downarrow}. \quad (2)$$

The rates can be expressed in terms of p as¹³

$$\tau_{\text{DMA}} = \tau_1 \frac{\sqrt{1-p^2}}{2}, \quad (3a)$$

$$\tau_\uparrow = \tau_1 \sqrt{\frac{1+p}{1-p}}, \quad (3b)$$

$$\tau_\downarrow = \tau_1 \sqrt{\frac{1-p}{1+p}}, \quad (3c)$$

where $\tau_1 = \tau_{10} \exp(E_1/k_B T)$. Here E_1 is the activation energy for the DMA reorientation in the symmetric ($\Delta=0$) potential and the “up” and “down” rates obey the detailed balance condition; $\tau_\uparrow/\tau_\downarrow = \exp(\Delta/k_B T)$. The DMA reorientations are considered to be rather slow and are expected to freeze out at the phase transition temperature, yielding a static dielectric polarization below $T_c = 152$ K.

The other dynamic processes in DMAAS are considered to be much faster and do not freeze at T_c . These are the intra-H-bond motions of the O-H \cdots O and N-H \cdots O protons in the H-bond double-well potentials and the 120° CH₃ and 180° H₂O reorientations. We assume that these processes can be characterized by an autocorrelation time $\tau_2 = \tau_{20} \exp(E_2/k_B T)$. Which one of these actually dominates the proton relaxation will be estimated by a comparison of the magnitude of the relaxation rates to the theoretical values obtained for a given molecular structure and geometry.

The proton spin-lattice relaxation rate $(T_1)^{-1}$ is obtained by summing up the spectral densities of the autocorrelation functions for both kinds of motions

$$\frac{1}{T_1} = A(1-p^2) \frac{\tau_{\text{DMA}}}{1+(\omega_0 \tau_{\text{DMA}})^2} + B \frac{\tau_2}{1+(\omega_0 \tau_2)^2}. \quad (4)$$

Here $1-p^2$ is the “depopulation” factor¹⁴ due to the asymmetry of the DMA potential and ω_0 is the nuclear Larmor frequency. Within the same model of randomly fluctuating local magnetic fields one obtains the relaxation rate in the dipolar frame $(T_{1D})^{-1}$ as¹⁵

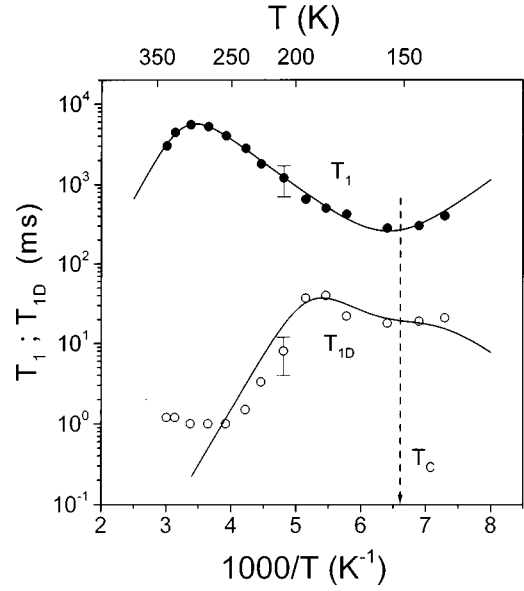


FIG. 2. Temperature dependence of the proton spin-lattice relaxation time T_1 (solid circles) and the proton relaxation time in the dipolar frame T_{1D} (open circles) of a DMAAS powder specimen. Solid lines represent fits with Eqs. (4) and (5).

$$\frac{1}{T_{1D}} = C(1-p^2) \left(\tau_{\text{DMA}} + \frac{5\tau_{\text{DMA}}}{1+(\omega_0 \tau_{\text{DMA}})^2} \right) + D \left(\tau_2 + \frac{5\tau_2}{1+(\omega_0 \tau_2)^2} \right). \quad (5)$$

The prefactors A , B , C , and D are treated as fit parameters in the fitting procedure.

The proton spin-lattice relaxation time T_1 of a DMAAS powder specimen was measured as a function of temperature at a frequency $\nu_0(^1H) = 32$ MHz. On cooling from 350 K T_1 first increases and exhibits a maximum at $T = 292$ K. Below that temperature it decreases continuously (Fig. 2) and exhibits a minimum around 156 K, thus slightly above T_c . Such a behavior can be explained by Eq. (4) which predicts two minima (occurring at $\omega_0 \tau_{\text{DMA}} = 1$ and $\omega_0 \tau_2 = 1$) in the temperature dependence of T_1 as a consequence of the presence of two dynamic processes on different time scales that both slow-down on cooling. The minimum at higher temperature is produced by the slower of the two motions. This minimum in fact occurs above our highest measured temperature so that only the increasing (slow-motion) part of the T_1 vs $1/T$ curve was detected between 350 and 292 K. The measurements were not extended to higher temperatures because the crystal starts to decompose by losing the crystalline water. Below 290 K the faster motion slows down to the extent that it produces another minimum at 156 K. This minimum occurs at $\omega_0 \tau_2 = 1$ and the Arrhenius analysis yields $\tau_{20} = 7.0 \times 10^{-13}$ s and $E_2 = 119 \pm 5$ meV. The same value of the activation energy was determined also in the dielectric relaxation study.⁹ It is interesting to calculate the value of τ_2 at the phase transition temperature 152 K. We obtain $\tau_2 \approx 10^{-9}$ s which demonstrates that this motion can not be associated with the order-disorder freezing at the FE transition as it is too fast to yield a static dielectric polarization at T_c . It corresponds to other degrees of freedom of the

DMAAS structure. One such possibility are 180° “jump-over” motions of water molecules in the Al(H₂O)₆ complexes, which were detected by the Raman spectroscopy.² The E_2 value of 119 meV is somewhat higher than that characterizing the proton motion within a double-well potential of a hydrogen bond (proton intra-H-bond motion) in H-bonded dielectrics like the KDP family where the activation energy was typically found in the range 70–80 meV. It is thus not very likely that the proton intra-H-bond motion would determine the τ_2 process. The contribution of the CH₃ rotations can however not be excluded.

Whereas the parameters of the τ_2 motion could be determined rather precisely from the T_1 data, the determination of τ_{DMA} from T_1 is much less precise. T_1 probes the dynamics in the 10⁷ Hz frequency observation window whereas the DMA dynamics is considerably slower and influences the T_1 only little. It is thus desirable to make another observation of the same system with a technique that probes the dynamics on a slower experimental time scale. Such a possibility is provided by the proton dipolar relaxation time T_{ID} , which is sensitive to molecular motions in the kHz range, thus four orders of magnitude slower than T_1 . T_{ID} is conveniently measured by the Jeener-Broekaert pulse sequence¹⁶ which transfers the high-field Zeeman spin order into the dipolar order by the application of a pair of phase-shifted rf pulses. In this way the dipolar energy reservoir is efficiently cooled resulting in a very low spin temperature. The evolution of the dipolar spin temperature towards the equilibrium then proceeds with the time constant T_{ID} . The change of the spin temperature is induced by the transitions between the energy levels of the proton magnetic dipole moments in the dipolar fields of their neighbors and the transition frequencies fall into the kHz frequency range.

The proton T_{ID} of DMAAS is displayed in Fig. 2. Between 330 and 230 K T_{ID} is weakly temperature dependent and has a rather short value of 1 to 1.5 ms indicating the presence of molecular dynamic processes with frequencies within the kHz range. A shallow minimum is observed at 260 K followed by a rapid increase below, so that T_{ID} reaches the value of 36 ms at 180 K. Below that temperature T_{ID} starts to decrease again. The parameters of the τ_{DMA} motion were extracted from the simultaneous fit of T_1 and T_{ID} with Eqs. (4) and (5) using the predetermined τ_{20} and E_2 values. The experimental data could be well reproduced (solid lines in Fig. 2) by the parameters $\tau_{10}=2.9\times 10^{-9}$ s, $E_1=67\pm 5$ meV and $\Delta=228\pm 10$ meV for the DMA motion. The fit of T_1 is excellent in the whole temperature range, whereas the above model fails to reproduce T_{ID} at temperatures higher than 250 K, probably due to the crudeness of the approximations used.

At the phase transition temperature 152 K the above parameter values yield the average “dwell” times $\tau_{\uparrow}=2.98\times 10^{-3}$ s and $\tau_{\downarrow}=8\times 10^{-11}$ s, so that the DMA molecule spends practically all the time in the lower energy state and is observed static in the NMR spectroscopic observation. At room- T , on the other hand, the motion is considerably faster; $\tau_{\uparrow}\approx 10^{-6}$ s and $\tau_{\downarrow}\approx 10^{-9}$ s; so that it is reasonable to associate this motion with the DMA reorientation freeze-out, yielding a static dielectric polarization below T_c . The value of the bias energy $\Delta=228$ meV should be regarded as a qualitative estimate only. It yields the occupancy of the

lower two degenerate energy states E_a of the DMA molecule at room- T of 99%, whereas the x-ray study¹ has estimated this to be about 80%. Further study is necessary to clarify this discrepancy.

There still remains the question on which motion is responsible for the minimum in T_1 at 156 K. Since the T_1 value in the minimum is actually independent of any value of the autocorrelation time and thus model-independent, it is possible to compare the T_1 value in the minimum to the theoretical values obtained for various types of proton relaxation mechanisms. For the 180° flips of water molecules in the Al(H₂O)₆ complexes we take in a crude estimate the water molecules as isolated with the H-H distance of 0.154 nm (i.e., the O-H distance 0.0975 nm and the O-H-O angle 105°). For well defined pairs of interacting protons we use the exact dipole-dipole formula derived for the random molecular jumps and reorientations¹⁷

$$\frac{1}{T_1} = \sum_{i<j} \frac{3}{10} \frac{\gamma^4 \hbar^2}{r_{ij}^6} \left\{ \frac{\tau_c}{1 + \omega_0^2 \tau_c^2} + \frac{4\tau_c}{1 + 4\omega_0^2 \tau_c^2} \right\}, \quad (6)$$

where r_{ij} is the interproton distance, γ the gyromagnetic ratio and τ_c the autocorrelation time for the H₂O reorientations. In the minimum ($\omega_0 \tau_c = 0.65$) we get the theoretical value $(T_1)_{\text{H}_2\text{O}} = 12$ ms which is a factor 20 shorter than the experimental value of 250 ms. A similar calculation for the CH₃ reorientations using the C-H distance of 0.109 nm and the H-C-H angle 107.1° yields $(T_1)_{\text{CH}_3} = 13$ ms whereas the NH₂ reorientations (the N-H distance 0.134 nm and the H-N-H angle 93.3°) yield $(T_1)_{\text{NH}_2} = 50$ ms. All these theoretical values are too short. It is very likely that the above molecules move in an asymmetric potential due to the crystalline electric fields so that one would have to include a depopulation factor $1-p^2$ in Eq. (6), which would make T_1 longer. Unfortunately the actual potential shapes for the molecules of the DMAAS structure are not known so that a quantitative analysis cannot be made. The dominant relaxation mechanism can thus not be identified in a simple way. There exists in addition also spin-diffusion among protons that actually mixes all the relaxation pathways.

III. ²⁷Al NMR

Protons interact predominantly among themselves via the magnetic dipole interaction whereas the coupling to the rest of the lattice is relatively weak. Structural displacements of the lattice ions have thus little effect on the proton resonance so that the information obtained from protons is not very site-specific. A much more site specific study is provided by the ²⁷Al NMR. ²⁷Al is a quadrupolar nucleus (spin $I=5/2$) and its electric quadrupole moment interacts with the electric field gradient (EFG) tensor produced by the charges of the surrounding ions and electrons. Static displacements of the atoms change the EFG at the aluminum sites and affect the position and shape of the ²⁷Al NMR spectral lines. Dynamic components of the atomic displacements produce, on the other hand, spin-lattice relaxation via the time-fluctuating electric quadrupole interaction. The largest contribution to the EFG at the Al sites comes from the closest electric charges, which are the six water molecules octahedrally coordinated around a given Al atom. As these water molecules

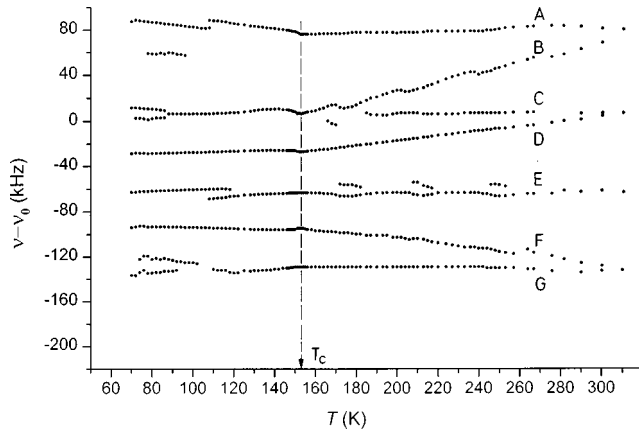


FIG. 3. Temperature dependence of the ^{27}Al NMR spectral line positions in a DMAAS monocrystal [$\nu_0(^{27}\text{Al}) = 26.134 \text{ MHz}$].

form hydrogen bonds with the surrounding SO_4 tetrahedra, the ^{27}Al nuclei see the static distribution of H-bond charges (the ^{27}Al spectrum) and the H-bond dynamics (the ^{27}Al spin-lattice relaxation rate). Since one oxygen of each H bond is located on the SO_4 molecule, the ^{27}Al sees also the deformations of the SO_4 tetrahedra which may occur as a result of the DMA freeze-out dynamics. The DMA molecules are coupled to the SO_4 via the N-H \cdots O bonding and the freezing of the DMA reorientations results in a static deformation of the SO_4 tetrahedral geometry.

A. ^{27}Al NMR spectrum and the double resonance experiment

The ^{27}Al NMR spectrum (central transition) has been measured in a DMAAS monocrystal as a function of temperature. The crystalline c axis was positioned perpendicular to the magnetic field and the crystal was rotated to such an orientation that all the spectral lines appeared resolved. According to the crystal structure, two ^{27}Al resonance lines are expected at room temperature for a general crystal orientation. There are namely two Al sites in the unit cell which were reported to be related by a twofold symmetry axis¹ (parallel to b). This symmetry requires the two Al EFG tensors to be chemically equivalent but physically inequivalent. At 310 K we found however four lines in the NMR spectrum instead of expected two (Fig. 3). The reason is the domain structure of DMAAS consisting of twin domains^{6,7} in the m -plane with the twist angle of 20.4° . The domains are created under external stress and stay in the sample indefinitely after creation. The twinning doubles the number of resonance lines so that four lines are observed instead of two. In order to verify that there are really only two Al sites in the unit cell we performed a double resonance experiment¹⁸ where the pure zero-field ^{27}Al quadrupole resonance (NQR) lines are detected indirectly via the protons. NQR is insensitive to the different orientation of the domains so that it yields the number of sets of three resonance lines equal to the number of chemically inequivalent ^{27}Al sites in the unit cell. In the double resonance experiment the nuclear spins are first polarized in a high magnetic field (0.8 T) and then adiabatically demagnetized in the laboratory frame to a low field (0.6 mT). This efficiently cools the spins which acquire a very low spin temperature. The sample is kept in the low magnetic field for a certain time and is irradiated by a radio-

frequency field of various frequencies. Whenever the frequency of the rf field matches one of the three frequencies of the ^{27}Al zero-field quadrupolar transitions, the Al nuclei absorb the rf energy and their quadrupolar energy reservoir is heated. Due to a magnetic dipolar coupling between the ^{27}Al and ^1H nuclei, the energy flows from the hot ^{27}Al to the cold proton subsystem and the proton spin temperature raises. This is detected as a drop in the proton magnetization after the adiabatic remagnetization. The drop is detected every time the frequency of the rf field matches one of the ^{27}Al quadrupolar transitions. The experiment was performed at 183 K as only there the proton dipolar relaxation time was long enough. Three transitions were found for the Al(1) site with the frequencies 275, 535, and 810 kHz (corresponding to $\pm 1/2 \leftrightarrow \pm 3/2$, $\pm 3/2 \leftrightarrow \pm 5/2$, and $\pm 1/2 \leftrightarrow \pm 5/2$ transitions) and 360, 690 and 1050 kHz for the Al(2) site. The corresponding quadrupole coupling constants and the asymmetry parameters are $e^2qQ/h = 1790 \pm 20 \text{ kHz}$ and $\eta = 0.15 \pm 0.1$ for the Al(1) site and $e^2qQ/h = 2315 \pm 20 \text{ kHz}$ and $\eta = 0.18 \pm 0.1$ for the Al(2) site. The quadrupolar transitions could be assigned rather unambiguously to the ^{27}Al nuclei due to a large width of the double resonance lines resulting from a large ^{27}Al magnetic dipole moment. In the sample there are also ^{14}N nuclei whose frequencies lie in the same range as those of ^{27}Al . However, due to a small ^{14}N magnetic dipole moment, their resonance lines would be much narrower and weaker. In addition, in the weak magnetic field of the double resonance experiment the dipolar coupling of integer spin ^{14}N ($I=1$) nuclei to protons is greatly reduced due to the ‘‘spin quenching’’ effect¹⁹ and the ^{14}N lines can not be easily observed. The double resonance experiment shows that there are two Al sites in the unit cell at the temperature 183 K. The fact that these two sites are chemically inequivalent (different e^2qQ/h and η) demonstrates that the local symmetry of the Al sites is lower than reported.¹ Were the Al sites related by a twofold or a twofold screw axis, their EFG tensors would be chemically equivalent (the same EFG tensor eigenvalues), but physically inequivalent (different orientations of the eigenvectors), resulting in a single set of Al transitions in the double resonance experiment. In view of the rather close e^2qQ/h and η values of the two Al sites, the reported twofold symmetry is however approximately obeyed and can be considered as a pseudo-twofold symmetry. It is likely that this pseudo-twofold symmetry detected at 183 K (i.e., relatively close to T_c) becomes an exact twofold symmetry due to the motional averaging effects at higher temperatures.

The temperature dependence of the resonance line positions in the ^{27}Al spectrum has been measured between 310 and 70 K with a high temperature resolution in steps of 1 to 2 K (Fig. 3). Each of the four Al lines observed at 310 K gradually splits into two already few degrees below that temperature. The eight ^{27}Al lines show a different temperature dependence on cooling. The positions of some of the lines show a monotonic change whereas the others show an unusual behavior. This is especially pronounced on the lines labeled B and E which are shown on an expanded frequency scale in Fig. 4. The position of the line B [Fig. 4(a)] shows unusual dips in the paraelectric phase at temperatures approximately 242, 207, and 169 K. The line E, on the other hand, splits three times into two lines in a way that one line

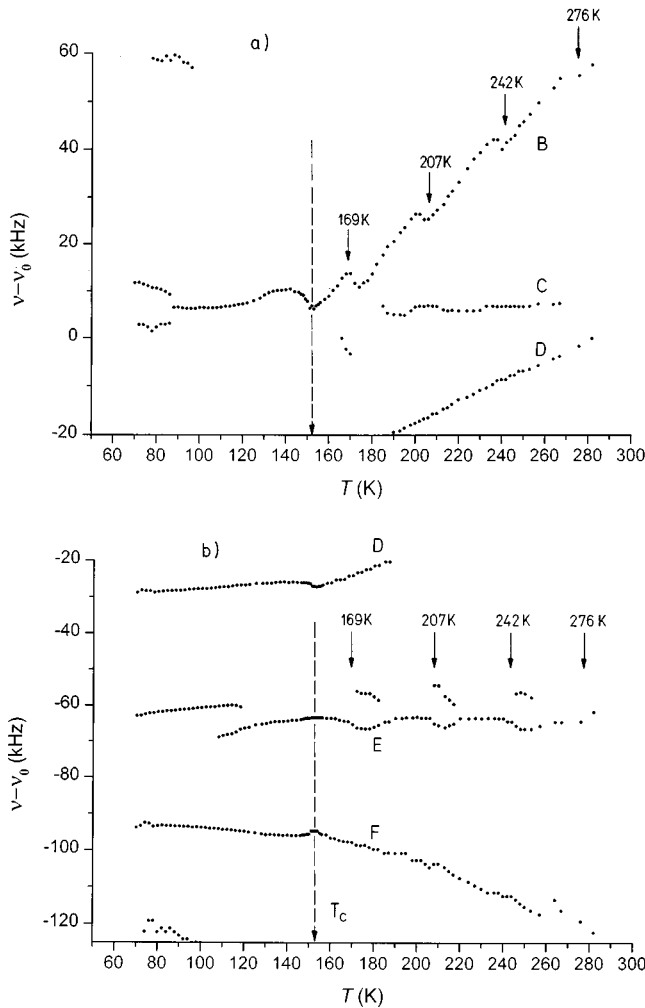


FIG. 4. Temperature dependence of the lines *B* (a) and *E* (b) from Fig. 3 displayed on an expanded frequency scale. The arrows indicate the temperatures where the minima of the ^{27}Al spin-lattice relaxation rate (Fig. 5) occur in the paraphase.

appears at a slightly shifted position and increases in intensity whereas the other decreases in intensity and gradually disappears. The temperatures of the anomalies in the lines *B* and *E* are related. At the positional minima of the line *B* the doublet structure of the line *E* disappears. At the ferroelectric transition temperature 152 K no marked changes in the spectral lines are observed. At T_c some of the lines show an insignificant continuous change in frequency whereas the others pass T_c smoothly. Going below T_c into the FE phase further discontinuous changes are observed between 115 and 105 K on two lines *A* and *E*, where again one line gradually disappears and a new one appears slightly shifted in frequency. The lines *B* and *E* show another change at about 90 K, where each of these two lines splits into a doublet which does not vanish on further cooling.

The observed changes of frequencies of the ^{27}Al spectral lines directly reflect the static changes of the EFG tensor at the position of the Al nuclei on cooling. These changes are a consequence of the static positional displacements of the charged ions in the vicinity of the Al sites. In Fig. 3 it is clearly observed that the static rearrangement of atoms in the DMAAS structure is as a continuous process starting already at room temperature which is as much as ~ 260 K above the

ferroelectric transition. This process shows practically no discontinuity at T_c . Since the dielectric data indicate rather unambiguously that the phase transition is connected with the DMA reorientations freeze-out, the following explanation of the ^{27}Al NMR spectrum can be given. The DMA molecules themselves do not contribute significantly to the Al EFG tensor due to a relatively large distance between the DMA and the $\text{Al}(\text{H}_2\text{O})_6$ complex. The EFG is determined predominantly by the charges of water molecules and the H-bonded oxygens of the SO_4 tetrahedra. The changes of the NMR spectrum reflect the change of geometry of the H-bond network and the associated distortions of the SO_4 tetrahedra. The above changes are induced by the gradual freeze-out of the DMA molecules which lower the local crystal symmetry, so that the potential in which the water molecules move, becomes biased. This biasing restricts the freedom for the H_2O 180° flips so that the water molecules gradually freeze on cooling. Similarly the biasing of the potential can produce also the slowing-down of the proton intra-H-bond motion. The above hypothesis requires that the DMA reorientations above T_c are slow or comparable to the NMR spectrum frequency scale (which is in the ten kHz range) in order that the changes of the spectral line positions appear static. Such slow dynamic processes were indeed observed in the above described proton T_{1D} experiment. The ^{27}Al NMR spectrum thus reflects the complicated interplay between the DMA, SO_4 , and $\text{Al}(\text{H}_2\text{O})_6$ H-bonded sublattices. A slowing-down of the DMA motion induces gradual structural rearrangements in the other two sublattices, so that all structural elements adjust to each other in an energetically favorable way. Despite some similarity with phase transitions [e.g., the behavior of the line *E* in Fig. 4(b) resembles a sequence of three first-order phase transitions] this process cannot be regarded as a sequence of macroscopic phase transitions as no associated changes of the average crystal symmetry were observed so far.

B. ^{27}Al spin-lattice relaxation

In order to obtain more information on the dynamics of the DMAAS system, a ^{27}Al spin-lattice relaxation experiment has been performed. Measurements were made on a DMAAS monocrystal at a frequency $\nu_0(^{27}\text{Al})=26.134$ MHz. The inversion-recovery method was used to determine the spin-lattice relaxation rate. There are two spin transition probabilities W_1 and W_2 involved in the ^{27}Al electric quadrupolar relaxation, corresponding to the $\Delta m = \pm 1$ and $\Delta m = \pm 2$ changes of the magnetic quantum number. W_1 and W_2 were extracted from the magnetization-recovery curve using the standard analysis²⁰ for spin $I=5/2$. Since W_1 and W_2 behave with temperature in a completely analogous way, only W_1 is discussed in the following. Temperature dependence of W_1 was measured from 310 to 70 K from the Fourier-transformed spectra on the line *E*. This line was chosen in order to throw some more light on the nature of the unusual splittings found at three temperatures in the paraphase. W_1 is shown in Fig. 5 where a typical slowing-down behavior on cooling is observed. The inverse transition probability W_1^{-1} (loosely speaking the spin-lattice relaxation time T_1) decreases from room temperature down to T_c . At 152 K W_1^{-1} exhibits a global minimum and starts to increase

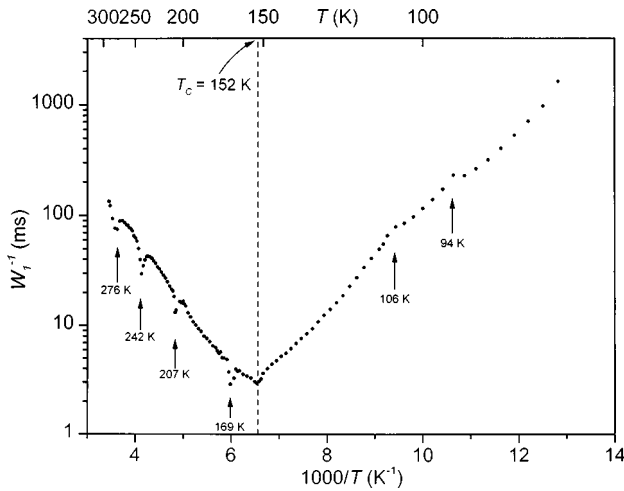


FIG. 5. Temperature dependence of the ^{27}Al spin-lattice relaxation rate W_1^{-1} of DMAAS measured on the line E [shown in Fig. 4(b)].

on further lowering the temperature. In the paraphase the experimental points generally follow a straight line in the $\log W_1^{-1}$ vs $1/T$ plot. In addition four other minima are observed in the paraphase at temperatures 276, 242, 207, and 169 K. These are the same temperatures at which the anomalies in the line E are observed in Fig. 4(b) (the anomaly at 276 K was in fact not observed in the spectral line position due to a too large temperature increment in the measurement). Below T_c the experimental points again follow a straight line with approximately the negative slope of the high- T part. Two additional discontinuities are observed at 106 and 94 K which coincide with the anomalies observed in the lines A , B , and G at these temperatures. Here it is worth mentioning that around 105 K small anomalies were detected also in the other physical parameters, the crystal elasticity,⁶ the dielectric constant,¹⁰ and the spontaneous polarization.⁸ It was however shown that no new components in the spontaneous polarization appear at that temperature so that the anomalies cannot be associated with a macroscopic ferroelectric phase transition.

The spin-lattice relaxation data allow to extract the auto-correlation time τ_c for molecular motions producing the ^{27}Al spin-lattice relaxation in DMAAS. At the minimum τ_c equals to the inverse nuclear Larmor frequency, wherefore we get $\tau_c = 6 \times 10^{-9}$ s at T_c . Disregarding the four additional minima in the paraphase for the moment, the activation energy is obtained from the T_1 slope of the global minimum as $E_a = 115 \pm 5$ meV and $\tau_\infty = 6 \times 10^{-13}$ s. These values are within the experimental accuracy equal to those obtained for the τ_2 dynamic process in the proton T_1 analysis. This demonstrates that both nuclei, the protons and the ^{27}Al , see the same molecular motion. The short τ_c value of the order of 10^{-9} s at T_c again demonstrates that the detected motion is too fast to yield a static dielectric polarization in the ferroelectric phase and cannot be associated with the DMA freeze-out. We propose instead to associate this motion with the H_2O dynamics around a given Al atom and explain its slowing-down character by the gradual biasing of the local water potentials as a result of the DMA gradual freeze-out, which lowers the local crystal symmetry. Since there are many structurally different water molecules in the H-bond

network, they may experience different bias fields so that their reorientational motions freeze-out at different temperatures. The gradual H_2O freeze-out gives a possible explanation of the four minima in the temperature dependence of W_1^{-1} in the paraphase. The minima are rather sharp and resemble a local soft-mode slowing-down dynamics. As already stated, no macroscopic symmetry changes were detected so far at the temperatures of the minima.

There is still another puzzling question why the minimum in W_1^{-1} occurs exactly at T_c since it is evident that the slowing-down motion producing the ^{27}Al relaxation is not directly the DMA freeze-out but a much faster dynamic process. The answer can be given by a comparison of the ^{27}Al and the proton relaxation time minima. Proton relaxation time was measured at a frequency 32 MHz and the minimum in T_1 occurred at 156 K. The ^{27}Al T_1 was measured at 26.134 MHz and the minimum occurred at 152 K. Due to a slightly lower frequency the ^{27}Al minimum (of the Bloembergen-Purcell-Pound-type) was shifted to lower temperatures and accidentally coincides with the FE transition temperature. This can be verified by a simple calculation. Calculating τ_c with the above E_a and τ_∞ parameters for the temperature 156 K yields the resonance frequency from the condition for the minimum of the relaxation rate $\nu_0 = 1/(2\pi\tau_c) = 33$ MHz. Within the experimental accuracy this value agrees well with the actual proton resonance frequency 32 MHz.

IV. CONCLUSIONS

DMAAS is a representative of a family of inorganic hydrogen-bonded insulators where the H-bond network is considerably more complicated than in the commonly investigated families of $\text{K}_3\text{H}(\text{SO}_4)_2$, CsHSO_4 , squaric acid and KDP. Whereas the physical properties of the latter families can be to a good approximation explained by considering the H-bond network only, the origin of the ferroelectric ordering in DMAAS is more complicated and cannot be analyzed within the H-bond network substructure only. The ^1H and ^{27}Al NMR studies have demonstrated the existence of two kinds of molecular motions in the paraphase with frequencies which differ for about five orders of magnitude. The slow motion corresponds to the DMA reorientational dynamics which freezes-out at the ferroelectric transition whereas the fast motion reflects the dynamics of the H-bond network and shows no anomaly at T_c . The results demonstrate that the DMA rotation freeze-out is indeed the prime reason for the ferroelectric transition in DMAAS. The DMA slowing-down dynamics has a profound effect on the other two sublattices, the SO_4 and the $\text{Al}(\text{H}_2\text{O})_6$, via the hydrogen bonding. The effect of the relatively slow DMA reorientations is a gradual lowering of the time-average local crystal symmetry which biases the local potentials of the water molecules as well as of the H bonds. A consequence is a gradual freeze-out of the water dynamics in the paraphase which manifests in the appearance of four additional minima in the ^{27}Al spin-lattice relaxation rate. The additional splitting of the ^{27}Al spectral lines much below the FE transition temperature indicates that the proton ordering in the H bonds begins to take place below 90 K.

- *On leave from Department of Physics, Korea University, 136-701 Seoul, Korea.
- ¹L. F. Kirpichnikova, A. Pietraszko, K. Lukaszewich, L. A. Shuvalov, V. V. Dolbinina, and L. M. Yakovleva, *Crystallogr. Rep.* **39**, 990 (1994) [*Kristallografiya* **39**, 1078 (1994)].
- ²V. I. Torgashev, Yu. I. Yuzyuk, L. F. Kirpichnikova, L. A. Shuvalov, and E. F. Andreev, *Sov. Phys. Crystallogr.* **36**, 376 (1991) [*Kristallografiya* **36**, 677 (1991)].
- ³R. Sobiestianskas, J. Grigas, E. F. Andreev, and V. M. Varikash, *Phase Transit.* **40**, 85 (1992).
- ⁴S. Dacko and Z. Czaplá, *Ferroelectrics* **185**, 143 (1996).
- ⁵L. F. Kirpichnikova, A. Pietraszko, M. Polomska, G. A. Kiosse, B. Hilczer, E. F. Andreev, and L. A. Shuvalov, *Crystallogr. Rep.* **41**, 685 (1996) [*Kristallografiya* **41**, 722 (1996)].
- ⁶L. F. Kirpichnikova, A. A. Urusovskaya, V. I. Mozgovoi, G. A. Kiosse, and I. M. Razdobreev, *Sov. Phys. Crystallogr.* **36**, 859 (1991) [*Kristallografiya* **36**, 1516 (1991)].
- ⁷L. F. Kirpichnikova, L. A. Shuvalov, A. A. Urusovskaya, N. R. Ivanov, and G. A. Kiosse, *Ferroelectrics* **140**, 1 (1993).
- ⁸L. F. Kirpichnikova, N. R. Ivanov, N. D. Gavrilova, V. V. Dolbinina, G. L. Slabkova, and L. A. Shuvalov, *Sov. Phys. Crystallogr.* **36**, 702 (1991) [*Kristallografiya* **36**, 1241 (1990)].
- ⁹R. Sobestianskas, J. Grigas, V. Samulionis, and E. F. Andreev, *Phase Transit.* **29**, 167 (1991).
- ¹⁰V. Kapustianik, M. Bublyk, I. Polovinko, S. Sveleba, Z. Trybula, and E. Andreev, *Phase Transit.* **49**, 231 (1994).
- ¹¹J. Wolak, B. Hilczer, L. F. Kirpichnikova, and L. A. Shuvalov, *Crystallogr. Rep.* **40**, 994 (1995) [*Kristallografiya* **40**, 1069 (1995)].
- ¹²S. Woepke, G. Sorge, V. Mueller, H. Hempel, and L. A. Shuvalov, *Proceedings of the 19th Spring Conference on Ferroelectricity*, Martin-Luther-University, Halle-Wittenberg (Burgscheidungen, Germany, 1991), p. 121.
- ¹³N. Korner, ETH Zürich, Diss. ETH No. 9952, 1993 (unpublished), p. 54.
- ¹⁴D. C. Look and I. J. Lowe, *J. Chem. Phys.* **44**, 3437 (1966).
- ¹⁵M. Goldman, *Spin Temperature and Nuclear Magnetic Resonance in Solids* (Clarendon, Oxford, 1970), p. 59.
- ¹⁶J. Jeener and P. Broekaert, *Phys. Rev.* **157**, 232 (1967).
- ¹⁷A. Abragam, *The Principles of Nuclear Magnetism* (Oxford University Press, Oxford, 1960), p. 291.
- ¹⁸See, e.g., J. Seliger, in *Proceedings of the Ampere Summer Institute on Advanced Techniques in Experimental Magnetic Resonance* (Portorož, 1993), edited by R. Blinc, M. Vilfan, and J. Slak (J. Stefan Institute, Ljubljana, 1993), p. 55.
- ¹⁹G. W. Leppelmeier and E. L. Hahn, *Phys. Rev.* **141**, 724 (1966).
- ²⁰E. R. Andrew and D. P. Tunstall, *Proc. Phys. Soc. London* **78**, 1 (1961).